

Optical diffusion diagnostics of evolving polymer foams

© M.V. Alonova,¹ S.S. Volchkov,¹ D.A. Zimnyakov,² A.A. Isaeva,¹ E.A. Isaeva,¹ E.V. Ushakova,¹ O.V. Ushakova¹

¹Yuri Gagarin State Technical University of Saratov,

Saratov, Russia

Institute of Precision Mechanics and Control of the Federal Research Center „Saratov Scientific Center“ of RAS,

410028 Saratov, Russia

e-mail: zimnykov@mail.ru

Received December 19, 2022

Revised December 19, 2022

Accepted December 19, 2022

Various approaches to the optical diagnostics of evolving polymer foams formed as a result of a decrease in the external pressure according to a given scenario in the „polymer–supercritical fluid“ systems are considered. Formed polymer foams are considered as a material platform for the creation of scaffolds for biomedical applications. Diagnostics of the current state of the foam was carried out by statistical analysis of the spatiotemporal fluctuations of the probe laser radiation, multiple scattered in the volume of the evolving foam, or by analyzing the fluorescent response during foaming of the „polymer–fluorophore“ mixture, pumped by laser radiation in the absorption band of the fluorophore. A relationship has been established between the average lifetime of dynamic speckles in scattered laser light and a generalized parameter characterizing the foam expansion dynamics. It was also found that the waveguide effect in the walls of the formed pores has a significant influence on the fluorescent response of the evolving foam, leading to an increase in the characteristic dwell time of fluorescence radiation in the walls and, accordingly, to an increase in the contribution of the induced component to the fluorescent response.

Keywords: fluorescent response, speckle correlometry, polylactide, foaming, supercritical carbon dioxide.

DOI: 10.21883/TP.2023.04.55933.279-22

Introduction

Foamed liquid and solid materials are widely used in various fields of modern science and technology, from the creation of new functional materials with unique characteristics to applications in biomedicine and the food industry. This demand is due to the specific physical properties of foams as heterogeneous media with a high stochasticity of ensembles of interfacial boundaries. Starting with W. Thomson (Kelvin) [1] and J. Gibbs [2], numerous theoretical and experimental studies have been devoted to various fundamental and applied aspects of the formation, development, stability, and destruction of the foamed media structure. The number of appropriate publications is currently in the hundreds.

Among various applications of foamed polymers, their possible use as a basis for the creation of functional bioresorbable materials for tissue engineering and regenerative medicine (the so-called scaffolds) should be noted [3–6]. One of possible approaches to the formation of biocompatible highly porous polymeric materials with the required structural characteristics is to use the technology of foaming initial polymers preliminarily plasticized in an atmosphere of a supercritical agent (supercritical fluid (SCF) foaming) [7–9]. Usually, polylactide [10–12] or polycaprolactone [13–15] are used as initial bioresorbable polymers, and carbon dioxide is used as a plasticizing/foaming agent. The use of CO₂ as an SCF technological agent for foaming is due to its low toxicity, the possibility of repeated use, and rather mild pressure and temperature conditions for the

transition to the supercritical fluid state ($P_{GI} \approx 7.37$ MPa, $T_{GI} \approx 304.13$ K [16]). It should be noted that in the field of SCF synthesis of highly porous functional materials for biomedical applications, there is currently a paradoxical situation: the high level of development of the technology for the synthesis of polymer foams, on the one hand, and the lack of effective methods for monitoring the structural characteristics of the formed porous matrices directly in the foaming process, on the other hand. Largely, such a gap is due to technological difficulties in probing expanding foam in the working volume of a supercritical reactor, as well as the stochasticity and nonstationarity of its structure.

Accordingly, it is of interest to develop optical diffusion methods for monitoring the current structural state of synthesized polymer foams by probing the expanding foam volume with laser radiation directly in the working zone of a supercritical reactor. In this regard, the aim of the work was to develop the physical foundations and experimental verification of methods for optical diffusion probing of evolving polymer foams based on the effects of multiple dynamic scattering of probing radiation in the foam volume and the conversion of laser light into the fluorescent response of an evolving foam.

1. Experimental technique

Experiments on laser probing of developing polymer foams were carried out using the SCF technology for foaming granular samples of polylactic acid (polylactide).

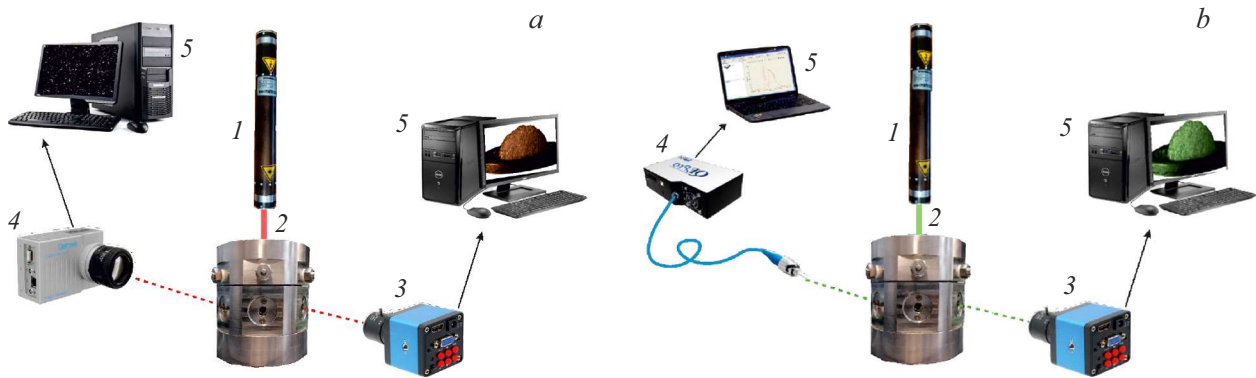


Figure 1. Schematic diagrams of experimental setups: *a* — for speckle-correlometric analysis of intensity fluctuations of radiation multiply scattered in an evolving foam volume. 1 — He–Ne laser; 2 — high-pressure multi-window reactor; 3 — CMOS camera 1; 4 — CMOS camera 2; 5 — PC; *b* — to study the fluorescent response of foam samples and starting materials; 1 — pulsed Nd:YAG laser ($\lambda = 532 \text{ nm}$); 2, 3, 5 — same as in Fig. *a*; 4 — Ocean Optics 65000 spectrometer with fiber optic patch cord.

The SCF procedure for the synthesis of highly porous polylactide matrices is based on preliminary plasticization of the initial material in an atmosphere of supercritical carbon dioxide for a specified time interval (from 30 min to 1 h) followed by pressure release in the working volume of the supercritical reactor according to a given scenario [8,17,18]. Upon completion of the plasticization step, a solution of carbon dioxide in the polymer is formed in the supercritical reactor, which is a thermodynamically stable single-phase system for constant values of pressure and temperature used in plasticization. A decrease in pressure leads to the transition of the polymer–carbon dioxide system across the binodal line in the „pressure–volume fraction of CO_2 in solution “ coordinate system and, accordingly, the appearance of an ensemble of pore nuclei (gas bubbles) in the solution [18]. In the process of pressure release, the size of the nuclei and their number increase, which at the macroscopic level manifests itself in an increase in the volume of the foamed system and an increase in the volume fraction of pores in the polymer matrix. At the final stage, the structure of the synthesized foam stabilizes as a result of hardening (vitrification) of the polymer matrix with a decrease in the concentration of carbon dioxide dissolved in it. A detailed analysis of the process of SCF foaming of polymers is presented in [19].

Foaming of polylactide PURASORB DL 04 (Corbion Purac, Netherlands, # 26680-10-4) was carried out in a multi-window supercritical stainless steel reactor in accordance with the procedure described earlier in Ref. [20]. Laser probing of the evolving foam (Fig. 1) was carried out using two approaches.

1) speckle-correlometric analysis of intensity fluctuations of He–Ne-laser radiation (GN-5P, $\lambda = 633 \text{ nm}$), multiply scattered in the evolving volume of foam; the expanding volume was illuminated with a laser beam through the top window of the reactor, and the scattered speckle-modulated laser light was recorded through the side window; Fig. 2 shows an example of a snapshot of a dynamic

speckle field selected from a video stream recorded by the Optronis3000x2 camera (position 3 in Fig. 1, *a*), and a time-synchronized snapshot of an evolving polylactide foam (ToupTec CAM1080PHB camera, position 4 in Fig. 1, *a*); analysis of the obtained speckle-correlometric data was carried out using estimates of the values of the average lifetime of dynamic speckles in the process of foam evolution [21]; details of the experiment and analysis of the obtained data are discussed in Section 3;

2) analysis of the spectral characteristics of the fluorescence response of an evolving foam preliminarily saturated with a fluorophore under conditions of fluorescence excitation by pulse-periodic laser radiation with a fixed power density. Rhodamine 6G was used as a fluorophore and excitation was performed by laser radiation with a wavelength of 532 nm; to increase the efficiency of the interaction of pump with fluorophore molecules distributed in the polymer matrix, in addition to rhodamine 6G, anatase nanoparticles were added to polylactide during plasticization. The details of preparation of fluorescent foam samples and excitation of a fluorescence response are discussed in Section 4.

2. Optical properties of foam as a randomly inhomogeneous medium

In the framework of the radiation transfer theory (see, e.g., [22]), a set of optical transport parameters of a randomly inhomogeneous medium is considered, which control the features of radiation propagation in the medium: the transport propagation length l^* , which characterizes the spatial scale of the transformation of a directed radiation flux into a diffuse one, the scattering length l , defined as the average distance traveled by the partial components of the scattered field in the medium between two successive scattering events, and the absorption length l_a , defined as the reciprocal of the medium absorption coefficient. In non-absorbing media $l_a \rightarrow \infty$, and the transport length

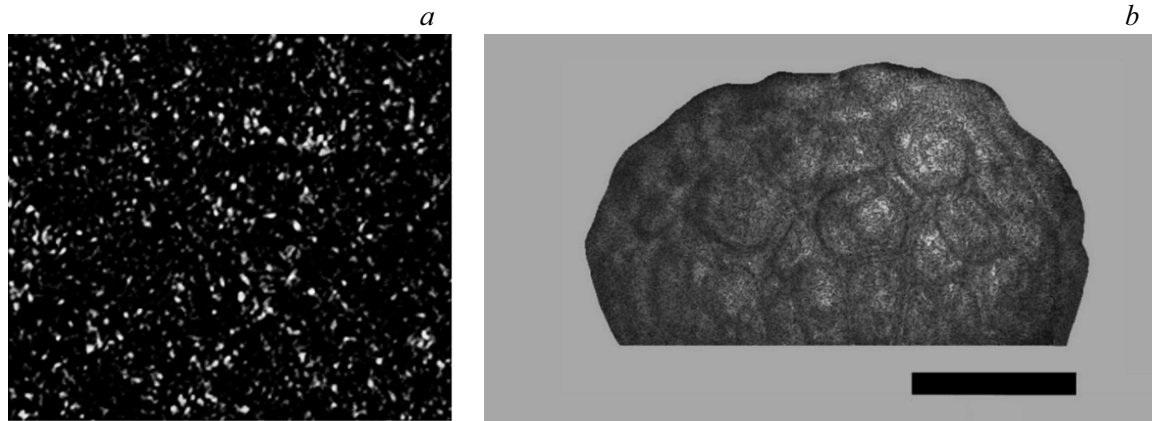


Figure 2. *a* — Example of a snapshot of speckle structure recorded by a CMOS camera 4 (Fig. 1, *a*; camera model Optronis 3000x2); exposure time 8ms; *b* — example of a snapshot of polylactide foam obtained using camera 3 (Fig. 1, *a*); pre-processing of the image (cleaning out the artifacts, correction of the background component) was carried out; the length of the black marker corresponds to 2 mm.

and the scattering length are related via the scattering anisotropy parameter $\bar{\mu}$: $l^* = l/(1 - \bar{\mu})$ [23]. Therefore, in the case of isotropic propagation of radiation in the medium ($\bar{\mu} \rightarrow 0$) $l^* \rightarrow l$, and in the presence of substantial anisotropy of scattering ($\bar{\mu} \rightarrow 1$) $l^* \gg l$. Non-absorbing foams occupy a special place among randomly inhomogeneous media due to the complex nature of the relationship between optical parameters and structural characteristics and the significant influence of the volume fraction of the condensed phase ε (polymer or liquid) on this relationship. In foam physics, it is customary to classify foamed substances depending on ε as wet foams ($\varepsilon > 0.2$), or dry foams ($\varepsilon < 0.05$). Wet foams can be considered in the standard approximation of weak scattering [22] as a macroscopically homogeneous scattering system consisting of a condensed medium (matrix) with randomly embedded scattering centers (gas bubbles). In evolving foams due to the change of a gradual transition occurs from the state of wet foam to the state of dry foam, which cardinally changes the scattering mechanism. In the intermediate region between the two states, the effect of optical inversion of the system takes place [23] (transition from the mode of scattering by gas bubbles in a condensed matrix to the mode of scattering by pore walls, wall crossings (Plateau–Gibbs channels) and nodes of the network formed by Plateau–Gibbs channels located in gas matrix).

An empirical relationship between the transport length, the average bubble diameter $\langle D \rangle$ and ε for foamed liquids, which makes it possible to adequately describe the optical transport properties of non-absorbing foams in a fairly wide range ε (from ≈ 0.02 to 0.36), was obtained by D. Durian et al. [24]:

$$l^* \approx \frac{\langle D \rangle}{\sqrt{\varepsilon}}. \quad (1)$$

Note that during SCF foaming of polymers at the stage of intensive expansion of the formed foam in the process of pressure relief, there is a significant increase in the

volume of the formed foam V_f with respect to the initial volume of the plasticized polymer V_p ; foam expansion factor $\Psi = V_f/V_p$ can reach 8–10 or more [20]. Using an approximate estimate for the foam volume $V_f \approx N_b \pi \langle D \rangle^3 / 6$ (N_b being the number of gas bubbles in the expanding foam, assumed N_b to change insignificantly during intensive expansion) and taking into account that $f \approx V_p/V_f$, we can conclude that upon intense expansion in the process of foaming $l^* \propto (\Psi)^{\frac{2}{3}}$ (i.e., within the framework of the assumptions used, the transport propagation length of the probing radiation in the evolving foam, increases approximately in proportion to the foam expansion factor). This feature must be taken into account when analyzing the results of laser probing of evolving polymer foams.

3. Speckle correlation monitoring of SCF synthesized polylactide foams

The speckle-correlometric analysis of non-stationary multiply scattering media is based on the well-known relationship between the parameters of the microscopic dynamics of scattering centers in the medium, its optical transport parameters (in particular, l^*), the probability density function $\rho(s, t)$ of the propagation paths of the partial components of the probing radiation in the medium, and the autocorrelation function of fluctuations of the strength $E(t)$ of the scattered light fields at the observation point [25,26]:

$$\begin{aligned} g_1(t, \tau) &= \frac{\langle E(t)E^-(t + \tau) \rangle}{\langle |E(t)|^2 \rangle} \\ &= \exp(-j\omega\tau) \int_0^\omega \exp \left\{ -\frac{1}{3} k^2 \langle \Delta r^2(t, \tau) \rangle \frac{s}{l^*(t)} \right\} \rho(s, t) ds. \end{aligned} \quad (2)$$

In Eq. (2), the superscript „ $-$ “ denotes complex conjugate, ω is the frequency of the probing radiation, $k = 2\pi/\lambda$ is the wave number of the probing radiation in the medium,

$\langle \Delta r^2(t, \tau) \rangle$ is the average square of the displacement of scattering centers in the medium during time τ characterizing their microscopic mobility and t determines the beginning of the interval of observing scattered field fluctuations with duration T . Note that Eq. (2) was obtained under the assumption that the multiply scattering medium is stationary, i.e., that there is no dependence on in the right-hand and left-hand sides of Eq. (2) and, accordingly, that l^* and the mobility of scattering centers are constant during the observation time. At the same time, it can also be applied to systems with weak nonstationarity, when T the conditions $\delta \langle |E(t)|^2 \rangle = \delta \langle I(t) \rangle \ll \langle I(t) \rangle$ and $\delta \langle I^2(t) \rangle \ll \langle I(t) \rangle^2$ hold, where $\delta \langle I(t) \rangle$ and $\delta \langle I^2(t) \rangle$ are variations of the first and the second statistical moments of speckle field intensity during the observation time. Obviously, this is true in the case, when during the interval T the following relations are valid: $\delta l^*(t) \ll l^*(t)$ and $\delta \langle \Delta r^2(t, \tau) \rangle \ll \langle \Delta r^2(t\tau) \rangle$. The dependence $l^*(t)$ (and, therefore, $\rho(s, t)$), as well as $\langle \Delta r^2(t, \tau) \rangle$ on time when assuming weak nonstationarity of the probed media implies their approximation by piecewise constant functions with values insignificantly changing at the time moments $t, t+T, t+2T, \dots$. The hypothesis of weak nonstationarity of the probed media and, therefore, the recorded dynamical speckle fields is applicable to study evolving foams by the speckle correlation method, since $\tau_{c,I} \ll T \ll \tau_{\text{exp}}$, where $\tau_{c,I}$ is the correlation time of intensity fluctuations for the recorded speckle patterns and τ_{exp} is the characteristic time of polymer foams expansion in the experiments.

We also note that Eq. (2) was obtained assuming that the probe radiation is monochromatic. At the same time, random fluctuations in the amplitude and phase of the probing radiation during the observation time lead to decorrelation of scattered quasi-monochromatic light over short time intervals even in the case of probing stationary media with fixed scattering centers. This trend manifests itself in a decrease in the contrast of the observed speckle patterns $\sigma_I(t)/\langle I(t) \rangle$ and, therefore, the modulus of time autocorrelation function $|g_1(t, \tau)|$ at small values of τ compared to the case of probing with monochromatic radiation. In Ref. [27] it was shown that when probing multiply scattering randomly inhomogeneous media with partially coherent light and recording the scattered radiation with a detector whose response time is considerably longer than the coherence time of the probing radiation, a criterion for significant impact of coherence on the statistical properties of the scattered light spatiotemporal fluctuations is the ratio $\langle |\Delta s| \rangle / l_c$. Here $\langle |\Delta s| \rangle$ is the mean absolute value of the difference of propagation path lengths of the scattered field partial components in the probed medium, l_c is the coherence length of the probing radiation. When $\langle |\Delta s| \rangle / l_c \leq 1$, a substantial suppression of the recorded intensity fluctuations occurs; in the limit $\langle |\Delta s| \rangle / l_c \rightarrow \infty$ we have $g_I(t)/\langle I(t) \rangle \rightarrow 0$, $|g_1(t, \tau)|_{t \rightarrow 0} \rightarrow 0$. When $\langle |\Delta s| \rangle / l_c \ll 1$, the effect of partial coherence is insignificant and $\sigma_I(t)/\langle I(t) \rangle \rightarrow 1$, $g_1(t, \tau)|_{\tau \rightarrow 0} \rightarrow 1$. In our case, the use of a GN-5P single-mode helium-neon laser with a

cavity length of about 30 cm as a radiation source, the small size of the scattering zone (the typical size of the synthesized foam samples at the final stage of expansion did not exceed 10 mm), and the used scheme for recording scattered radiation give reason to believe that $\langle |\Delta s| \rangle / l_c \ll 1$ and, therefore, the impact of partial coherence of the laser light is minor. This is also confirmed by the high contrast of the recorded snapshots of speckle patterns (Fig. 2, *a* and 3).

In speckle correlation experiments, as a rule, the normalized autocorrelation function of intensity fluctuations $I(t)$ at the observation point is determined rather than the normalized autocorrelation function of the field $g_1(t, \tau)$. Field and intensity correlations ($g_2(t, \tau) = \langle I(t)I(t+\tau) \rangle / \langle I(t) \rangle^2$) are related with $g_1(t, \tau)$ through the Siegert relation (see, e.g., [28]):

$$g_2(t, \tau) = 1 + \theta |g_1(t, \tau)|^2, \quad (3)$$

where the parameter $0 \leq \theta \leq 1$ is determined by the detection conditions (relation between the detector aperture size and the characteristic size of coherence domain, or the mean size of a speckle in the detection plane, as well as the parameter $\langle |\Delta s| \rangle / l_c$). From the experimentally measured $g_2(t, \tau)$ the modulus of $g_1(t, \tau)$ is then determined. A necessary condition for the validity of Eq. (3) is that the distributions of the random values of real and imaginary parts of the recorded speckle field $E(t)$ must be Gaussian with similar dispersions and zero mean values. As a rule, this is so in the case of multiple scattering of the probing laser light with deep stochastic modulation of phases in partial components of the scattered light field. Note that at $t = 0$ and $\theta = 1$ (perfect detection conditions) Eq. (3) corresponds to the fundamental property of random optical fields with the Gaussian statistics of the field strength: $\langle |E|^{2n} \rangle / \langle |E|^2 \rangle^n = n!$.

The traditional approach to speckle correlation analysis of the microscopic dynamics of scattering centers in the probed medium reduces to estimating the correlation time of multiply scattered field fluctuations τ_c corresponding to a decrease of $|g_1(t, \tau)|$ by e times. In this case, a priori information about the type of dynamics of scattering centers, e.g., in the case of Brownian dynamics of scatterers $\langle \Delta r^2(t, \tau) \rangle = 6D_s\tau$, where D_s is the coefficient of translation diffusion of scatterers. When a drift component dominates in the dynamics of scatterers $\langle \Delta r^2(t, \tau) \rangle = v_s^2\tau^2$, where v_s is the velocity of motion of scatterers in the multiply scattering medium. Accordingly, the estimation of the parameter of microscopic dynamics (diffusion coefficient D_s or velocity of drift motion v_s) from the correlation time τ_c obtained from the experimental data requires a priori knowledge about the character of motion of scattering centers. In the case of nonstationary media with complex structure and dynamics, such as the evolving foams considered, the interrelation between τ_c and the microscopic mobility of scatterers is substantially more complex as compared to the canonical cases of diffusion and drift microscopic dynamics. Moreover, the character of

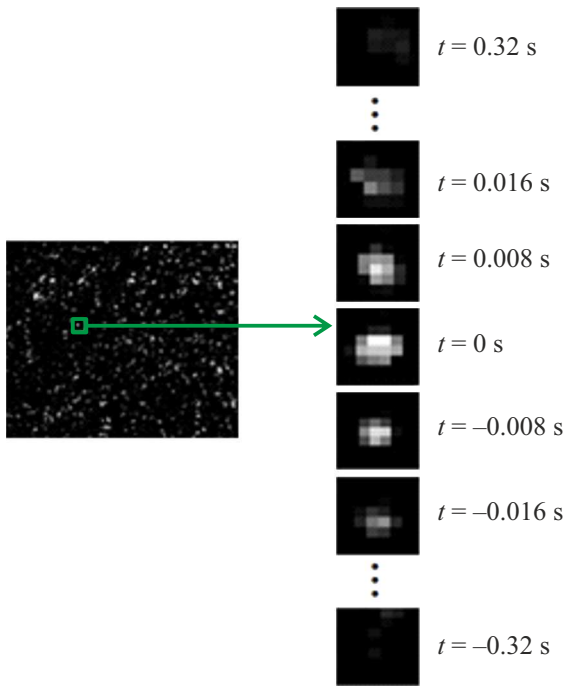


Figure 3. Technique for estimating the sample value of the lifetime of a dynamic speckle randomly selected in a sequence of images recorded by the Optronis camera (Fig. 1, *a*, position 4) during the synthesis of polylactide foam.

this interrelation can cardinaly change in the course of the system evolution.

Ref. [21] considers a different approach to the characterization of microscopic dynamics of scattering centers in nonstationary media using the experimental data on the characteristic time scales of laser radiation fluctuations. It was proposed to use as a characteristic time scale not τ_c , but the mean lifetime $\langle\tau_b\rangle$ of dynamic speckle in the recorded light field at the analyzed stage of the scattering system evolution. As a result of statistical modelling of multiple scattering of coherent radiation by scattering systems with different microscopic dynamics, it was found that $\langle\tau_b\rangle$ is independent of the microscopic dynamics type and determines the time interval, for which the condition $\sqrt{\langle\Delta r^2(t, \langle\tau_{li}\rangle)\rangle} \propto \lambda$ holds. As a result of modelling [21], it was found that under the conditions of multiple scattering of coherent radiation by a system of moving scattering centers the criterion of correspondence of the observation time interval Δt to the mean lifetime of dynamical speckles can be presented depending on the mean number N_{sc} of probe radiation scattering events as

$$\Delta t = \langle\tau_{li}\rangle \rightarrow \langle N_{sc} \rangle^{0.5} \sigma_\varphi = \Sigma_\varphi, \quad (4)$$

where σ_φ is the root-mean-square value of the phase shift per scattering event, Σ_φ is the critical total phase shift of partial components of the scattered field, constant for a system.

Figure 3 illustrates the technique of estimating a sample value of lifetime τ_{li} of a randomly chosen speckle by the

sequence of images of dynamic speckle structures, recorded by the Optronis camera in the course of polylactide foam formation. Using the set of obtained sample values of τ_{li} , the value of $\langle\tau_{li}\rangle$ averaged over the ensemble of dynamic speckles is then calculated for a given stage of evolution of the formed foam

Figure 4, *a* illustrates the dependences of the sample values of the mean lifetime of dynamic speckles on the volume of polylactide foam obtained from experimental data under various conditions of formation: with a slow pressure release ($dP/dt \approx 0.006$ MPa/s) in a supercritical reactor (data set 1) and in the case of fast release ($dP/dt \approx 0.03$ MPa/s, data set 2). The initial values of pressure and temperature in the supercritical reactor used in the plasticization of polylactide were equal to (8.2 ± 0.1) MPa and (318 ± 1) K. Estimation of the current values of the foam volume V_f in the process of pressure release in the reactor was carried out using sequences of snapshots of evolving foam, similar to Fig. 2, *b*, as described in [19]. The values of $\langle\tau_{li}\rangle$ were estimated for non-overlapping intervals of time as long as $T = 10$ s; also estimated was the mean rate of the foam volume increase $dV_f/dt = V_f'$ within the intervals as $V_f' \approx (V_{f,e} - V_{f,s})/T$, where the indices *s*, *e* denote the beginning and the end of the intervals.

Dependencies shown in Fig. 4, *a* can be interpreted within the framework of a phenomenological model that describes the relationship between the microscopic mobility of interfacial boundaries, which play the role of scattering centers in the foam volume, and the rate of the foam volume increase dV_f/dt . Let us assume that the pore (gas bubble) size averaged over the ensemble at the stage of intense foam expansion can be approximately represented as

$$\langle D \rangle \approx \left(\frac{K_c V_f}{N_c} \right)^{1/3}, \quad (5)$$

where K_c is the scaling factor determined by the shape of the pores (particularly, close to spherical), N_c is the number of pores in the foam volume. The increment $\langle D \rangle$ during the observation time Δt equals

$$\begin{aligned} \Delta \langle D \rangle &\approx \left\{ \left(\frac{K_c V_f}{N_c} \right)^{1/3} \right\}' \Delta t \\ &= \frac{K_c^{1/3}}{3} \left\{ \left(\frac{V_f}{N_c} \right)^{-2/3} \left(\frac{V_f' N_c - V_f N_c'}{N_c^2} \right) \right\} \Delta t. \end{aligned} \quad (6)$$

On the other hand, according to [21], there is an interrelation between the optical transport parameters of the evolving foam and the current mean size of a pore (see Eq. (1)): $l, l^* \propto \langle D \rangle$. Using the results of modeling [21], let us establish the interrelation between the characteristic size of the expanding foam L_f , the transport length of the radiation propagation through the foam l^* and the mean number of

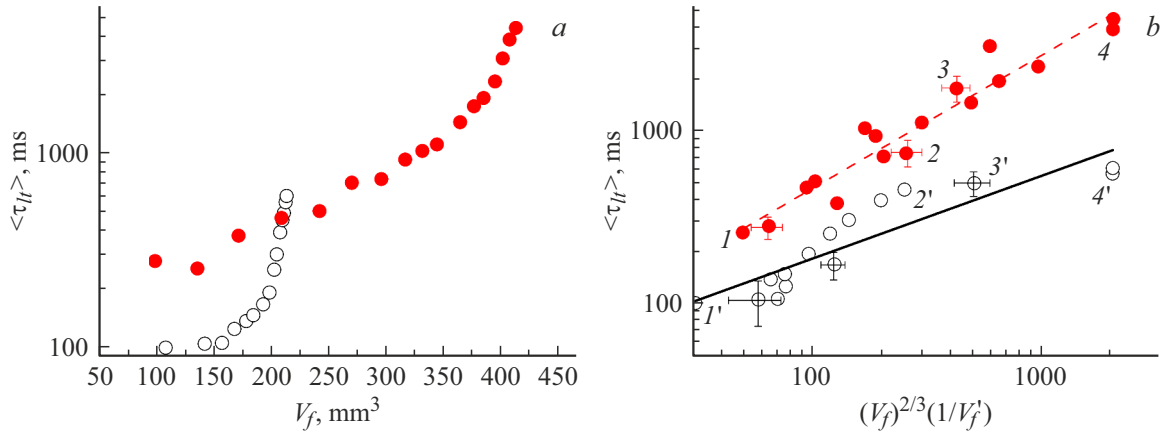


Figure 4. *a* — sample values of the average lifetime of dynamic speckles $\langle \tau_{lt} \rangle$ depending on the current volume of evolving polylactide foam at fast (○) and slow (●) pressure relief; *b* — dependence of $\langle \tau_{lt} \rangle$ on the parameter $V_f^{-2/3} \cdot V_f/dt$ in the case of slow (*bullet*) and fast (○) depressurization in the polylactide–carbon dioxide system. Time after start of depressurization: 1 — 365, 2 — 665, 3 — 975, 4 — 1215; 1' — 215, 2' — 605, 3' — 635, 4' — 665 s.

the probe radiation scattering events in the foam:

$$\langle N_{sc} \rangle \propto \left(\frac{L}{l^*} \right)^\beta, \quad (7)$$

where the exponent β is close to 1 in the mode of low-multiplicity scattering ($l^* \sim L$) and tends to 2 upon a transition to multiple scattering ($l^* \ll L$). Taking into account that $L \propto (V_f)^{1/3}$, $\langle D \rangle \propto (1/N_c)^{1/3}$, (expression (5)), and $l^* \propto \langle D \rangle$ (expression (1)), we get:

$$\langle N_{sc} \rangle \approx (N_c)^{\beta/3}. \quad (8)$$

On the other hand, we can assume that the root-mean-square phase shift per scattering event during the observation time Δt , caused by the interphase boundary dynamics in the expanding foam, is determined by the increment $\Delta \langle D \rangle$: $\sigma_\varphi \propto (2\pi/\lambda)\Delta \langle D \rangle$. Combining these relationships, we get the following phenomenological formula relating the average lifetime of dynamic speckles and the macroscopic characteristics of expanding foam:

$$\begin{aligned} \langle \tau_{lt} \rangle &\propto (N_c)^{-\beta/6} \left(\frac{V_f}{N_c} \right)^{2/3} \left(\frac{N_c^2}{V_f' N_c - V_f N_c'} \right) \\ &= (N_c)^{\frac{2-\beta}{6}} (V_f)^{2/3} \left(\frac{1}{V_f' - (V_f/N_c) N_c'} \right). \end{aligned} \quad (9)$$

Note that the key factor in this case is the time dependence of the number of cells (pores) N_c in the expanding foam. If the number of pores is constant or changing insignificantly (this case is characteristic of the „fast“ mode of expansion) $N_c' \approx 0$ and Eq. (9) reduces to a simpler form: $\langle \tau_{lt} \rangle \propto (V_f)^{2/3}(1/V_f')$, the right-hand side of which can be considered a generalized parameter $\Upsilon = (V_f)^{2/3}(1/V_f')$, reconstructed from empirical data on the foam expansion dynamics (see Fig. 4, *b*). The dependence of $\langle \tau_{lt} \rangle$ on

$(V_f^{2/3})(1/V_f')$ in the case of slow pressure release can be approximated by a linear function with acceptable accuracy (Fig. 4, *b*, $\langle \tau_{lt} \rangle \approx (1 \pm 1.4) \cdot \Upsilon^{4.22 \pm 0.42}$).

However, upon an increase in the rate of pressure release in the foam formation process, a noticeable deviation of experimental data from a linear dependence is observed; the interrelation between $(V_f)^{2/3}(1/V_f')$ and $\langle \tau_{lt} \rangle$ becomes approximated by the power dependence $\langle \tau_{lt} \rangle \approx (11.56 \pm 3.30) \cdot \Upsilon^{0.59 \pm 0.05}$ (Fig. 4, *b*). This feature can be explained by the influence of the number of pores in accordance with Eq. (9). Note that the increasing number of pores in the expanding foam doubly affects $\langle \tau_{lt} \rangle$. On the one hand, an increase in $\langle N_{sc} \rangle$ leads to a decrease in the mobility of scattering centers averaged over the ensemble, considered in terms of changing $\langle D \rangle$ during the time interval Δt (see Eq. (5)). On the other hand, increasing the number of cells in the foam must increase the mean value of the number of scattering events $\langle N_{sc} \rangle$ upon the propagation of the probe light through the foam volume and, accordingly, decrease the mean lifetime of dynamic speckles. Such an influence should be expected minor because of the small power exponent $\beta/6$. We can conclude (see Eq. (9)) that the increase in the number of pores with time partially decreases the influence of V_f' at positive values of $(V_f/N_c)N_c'$. Therefore, $\langle \tau_{lt} \rangle$ in the case of a fast pressure release, is characterized by slower growth with an increase in the foam volume as compared to the case of slow pressure release.

4. Analysis of the fluorescence response of SCF synthesized polylactide foams

As a possible approach to probing SCF synthesized polymeric foams, one can also consider the analysis of the spectral characteristics of the fluorescent response of foams saturated with fluorophores depending on the intensity

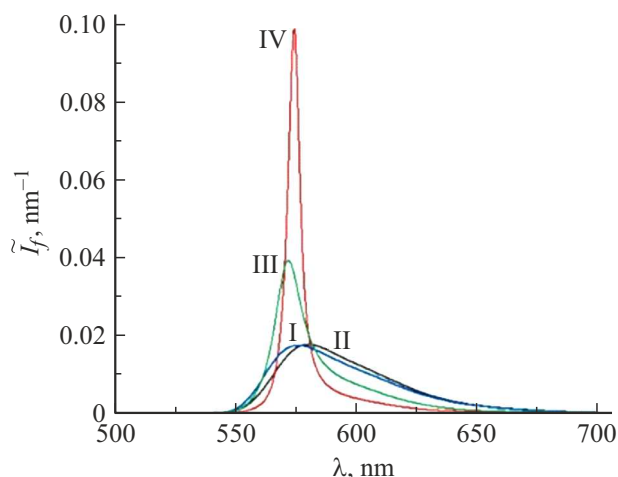


Figure 5. Normalized fluorescence spectra of the synthesized polylactide foam (I — $1.47 \cdot 10^5$; III — $4.7 \cdot 10^7$ W/cm²) and the initial polylactide/R6G/nanoparticles composite (II — $1.47 \cdot 10^5$; IV — $2.7 \cdot 10^7$ W/cm²).

of external laser pumping in the fluorophore absorption band [29]. This approach uses the effect of amplification of the induced component in a pumped multiply scattering medium when a certain level of population of the excited state of fluorophore molecules is reached. The enhancement of the induced component leads to a significant (up to 8–10 times) narrowing of the fluorescence response spectrum and is usually interpreted as a transition from spontaneous fluorescence in a medium to stochastic laser generation (random lasing, [30–32]). A characteristic feature of this transition is the saturation of the spectral response quality $Q_{ep} = \bar{\lambda}_f / \Delta\lambda_f$ ($\bar{\lambda}_f$ is the mean wavelength of the fluorescence response, is the FWHM of the fluorescence spectrum) at the levels of external laser pump substantially exceeding the conventional threshold of stochastic lasing, corresponding to $Q_{ep} = 2$. The saturation of the fluorescence spectral quality in a pumped medium is supposed to arise due to the achievement of the limit population of the excited state in the fluorophore molecules, determined by the ratio of the cross section of molecular stimulated emission to the cross section of radiation losses in the medium.

To study the spectral properties of the fluorescent response of SCF synthesized polylactide foams depending on the intensity of external pumping, polylactide PURASORB DL 04 used for foam synthesis was saturated with rhodamine 6G as a fluorophore. Anatase nanoparticles (product № 637254, Sigma Aldrich, USA) were added to the mixture of polylactide with a solution of rhodamine 6G in ethanol to increase the efficiency of the interaction of pump radiation with the fluorophore. The formed initial samples comprised 60 mg of polylactide, 60 ml of rhodamine 6G solution, and 10 mg of anatase nanoparticles. The samples were placed in cylindrical containers 11 mm in diameter and 1 mm high on glass substrates and preliminarily homog-

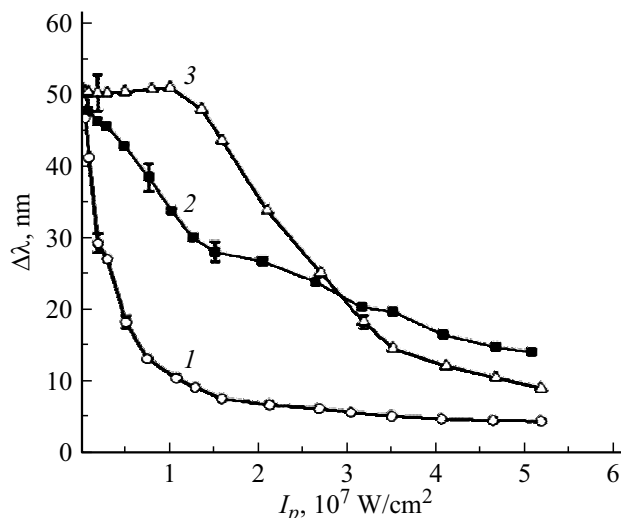


Figure 6. Typical dependencies ($\Delta\lambda = f(I_p)$) for homogenized starting materials (1, 3) and synthesized foam (2). The confidence intervals correspond to a confidence level of 0.9 and were determined for groups of five samples.

enized by heating to 333 K and gentle stirring for 600 s. Homogenized samples were introduced into a high-pressure SCF reactor (Fig. 1, b) and plasticized in an atmosphere of supercritical CO₂ (pressure: (8.2 ± 0.1) MPa temperature: (318 ± 1) K) during 1800 s. After that, the pressure in the reactor was released to a value of the order of 1 MPa at a rate of ≈ 0.02 MPa/s; further reduction of CO₂ pressure from 1 MPa to atmospheric pressure was carried out at a rate of ≈ 0.0015 MPa/s. It has been established that under such a mode of pressure release, the values of the foam expansion factor Ψ are approximately 5–6, and the sizes of the formed pores are in the range from ≈ 300 to ≈ 900 μ m.

The repetitively pulsed pumping of the initial samples and the synthesized polylactide foam was carried out by a beam of LOTIS TII 2134 ($\lambda_p = 532$ nm, beam diameter 5.0 ± 0.2 mm, pulse duration 10 ns, repetition rate 10 Hz, pump intensity changed from $1.5 \cdot 10^5$ to $5.2 \cdot 10^7$ W/cm² during the action of pulses). Fluorescence spectra of the samples were recorded through a fiber optical patchcord P100-2-UV-VIS with the Ocean Optics QE65000 spectrometer (position 4 in Fig. 1, b).

Figure 5 shows the normalized fluorescence spectra

$$I_f(\lambda, I_p) = I_f(\lambda, I_p) / \int_0^{\infty} I_f(\lambda, I_p) d\lambda \quad (10)$$

for the initial material (composite of polylactide, rhodamine 6G, and nanoparticles) and the synthesized polylactide foam at different pumping levels, clearly demonstrating the transition from purely spontaneous fluorescence to a significant contribution of the induced fluorescence component (stochastic lasing) in the pumped systems. Figure 6 illustrates the narrowing effect of the fluorescence response

spectra of the studied samples with increasing pump intensity.

In order to analyze the effect of the concentration of fluorophore molecules in the pumped volume on the transition from spontaneous fluorescence to stochastic lasing, we also obtained the dependence $\Delta\lambda(I_p)$ (Figure 6, curve 3) for the initial sample with fivefold decrease of the rhodamine 6G content (the volume of the solution of rhodamine 6G in ethanol was 12 ml). In this case, the concentration of fluorescence centers in the initial sample approximately corresponds to that in the foam synthesized using the initial samples with 60 ml of fluorophore solution averaged over the volume with the foam expansion factor taken into account. Note that the substantial narrowing of the spectrum for sample 3 is observed at much higher pumping levels compared to samples 1 and 2. At the same time, a smoother transition to the stochastic lasing mode and the absence of the spectrum width saturation at high pump intensities is characteristic of sample 2 as compared to samples 1 and 3.

The increase in the contribution of the induced component to the fluorescence response for the studied samples can be considered using estimates of the decay rate of the spectrum half-width $\Delta\lambda_f/\Delta I_p$ at low pump intensities. For the initial sample with 60 ml of fluorophore solution (Figure 6, curve 1), $\Delta\lambda_f/\Delta I_p$ has the maximum value ($\approx 1.07 \cdot 10^{-5} \text{ nm}/(\text{W}\cdot\text{cm}^2)$); for the synthesized foam $\Delta\lambda_f/\Delta I_p \approx 3.37 \cdot 10^{-6} \text{ nm}/(\text{W}\cdot\text{cm}^2)$, and for the sample with fivefold reduced fluorophore concentration $\Delta\lambda_f/\Delta I_p \approx 0$.

Such a behavior of the fluorescence response for the synthesized foam can be interpreted, on the one hand, within the framework of the concept of enhancement of the induced fluorescence component in randomly inhomogeneous media and, on the other hand, taking into account the features of radiation propagation in foamed media. The enhancement effect is characterized by the ratio of mean fluorescence radiation propagation length $\langle s \rangle$ in the pumped medium to characteristic scale l_{st} of propagation of partial components of the fluorescence field between successive induced emission events: $K = \langle s \rangle / l_{st}$ [29]. It should be expected that the amplification of the induced component in the medium is absent at $K \ll 1$ and reaches maximum values at $K \gg 1$. Characteristic length l_{st} can be presented as $l_{st} \approx (\sigma_{st} n_0 \langle f \rangle)^{-1}$, where σ_{st} is the cross section of induced emission for the fluorophore molecules, n_0 is their concentration in the pumped volume, $\langle f \rangle$ is the relative population of their excited state averaged over the pumped volume. The spectrum narrowing can be due to both an increase in $\langle s \rangle$ and a decrease in l_{st} . Upon the growth of pump intensity l_{st} , decreases due to the growing $\langle f \rangle$. Obviously, the limit value l_{st} of cannot be smaller than $l_{st} \approx (\sigma_{st} n_0)^{-1}$; in real pumped systems it turns to be greater due to the limitations of the maximum population $\langle f \rangle_{\max} < 1$ of the excited state.

A characteristic feature of radiation propagation in foamed media is the effect of photon channeling [33], which consists in the predominant propagation of both

pump and fluorescence radiation in the walls of pores and their intersection zones (Plateau–Gibbs channels). On the one hand, this leads to an increase in the average lifetime of fluorescence photons in the pumped volume compared to the initial materials and, accordingly, to an increase in $\langle s \rangle$. On the other hand, photon channeling of the pump radiation should lead to an increase in the pumped volume of the medium, a decrease in the average energy density of the pump field, and, accordingly, to a lower value of at high pumping intensities compared to the initial materials. Simultaneous increases in $\langle s \rangle$ and l_{st} when converting the starting material into a foamed structure oppositely affect the fluorescence response. We can suppose that it is this kind of competition that gives rise to observed features in the dependence $\Delta\lambda(I_p)$ for sample 2 (a large value of the parameter $\Delta\lambda_f/\Delta I_p$ and a substantially smooth transition from purely spontaneous fluorescence to the mode with a significant contribution of the induced component).

Conclusion

Thus, the considered approaches to optical diffusion monitoring of evolving polymer foams using laser radiation revealed some previously unknown fundamental features in the behavior of foamed polymer materials and in the interaction of probing laser and fluorescence radiation with them. In particular, the method of expanding foam laser probing an based on evaluating the average lifetime of dynamic speckles at different stages of expansion versus the current value of the foam volume and the rate of its increase allowed revealing the influence of such a factor, as the appearance and development of new pore nuclei in the polymer matrix at the stage of intense foam expansion. This factor can have a significant impact on the structural characteristics of the synthesized foam (the pore size average value and standard deviation, etc.) under certain conditions. As established by the analysis of the obtained experimental data, such a condition is a rapid pressure release in the reactor during foaming, giving rise to new pore nuclei in the polymer matrix during intense expansion of the foam. This is due to a significantly nonequilibrium (excessive) content of carbon dioxide in the matrix at the stage of intense foaming.

The study of the fluorescence response of polylactide foams saturated with a fluorophore (rhodamine 6G) as a function of the external laser pump intensity revealed a characteristic feature of converting laser radiation into fluorescence in such systems. This feature is a significantly higher than expected rate of narrowing the fluorescence spectrum with increasing pump intensity due to the so-called photon channeling. The photon channeling increases the characteristic residence time of fluorescence quanta in the polymer matrix and, accordingly, increases the probability of stimulated emission events. On the other hand, waveguide propagation of pump radiation in a polymer matrix can lead to a decrease in the volume-averaged

pump energy density and, accordingly, to a decrease in the population of the excited state of fluorophore molecules in the pumped system. It is the competition of these processes that leads to the experimentally observed behavior of the fluorescence response of the synthesized polylactide foams.

The considered approaches to laser probing of synthesized polymer foams and the results obtained can be used for further development of methods for optical diffusion diagnostics of multiply scattering media with a complex structure and dynamics.

Funding

The study was supported by the Russian Science Foundation, grant № 21-79-00051.

Conflict of interest

The authors declare that they have no conflict of interest.

References

- [1] W. Thomson (Lord Kelvin). *Philos. Mag.* **24** (151), 503 (1887). DOI: 10.1080/14786448708628135
- [2] J.W. Gibbs. *The Collected Works of J.W. Gibbs* (Longmans, NY., 1931), v. 1.
- [3] H.Y. Kweon, M.K. Yoo, I.K. Park, T.H. Kim, H.C. Lee, H.-S. Lee, J.-S. Oh, T. Akaike, C.-S. Cho. *Biomaterials*, **24** (5), 801 (2003). DOI:10.1016/S0142-9612(02)00370-8
- [4] R. Langer, J.P. Vacanti. *Science*, **260** (5110), 920 (1993). DOI:10.1126/science.8493529
- [5] D.W. Huttmacher. *Biomaterials*, **21** (24), 2525, (2001). DOI:10.1016/S0142-9612(00)00121-6
- [6] R. Lanza, R. Langer, J.P. Vacanti. *Principles of Tissue Engineering: Fourth Edition* (Elsevier Acad., GA, 2014)
- [7] A.I. Cooper. *Adv. Mater.*, **15**, 1049 (2003). DOI:10.1002/adma.200300380
- [8] R.L. Reis, A.R.C. Duarte, J.F. Mano. *J. Supercrit. Fluids*, **54** (3), 281 (2010). DOI: 10.1016/j.supflu.2010.07.013
- [9] E.N. Antonov, V.N. Bagratashvili, I.A. Borschenko, B.N. Khlebtsov, N.G. Khlebtsov, S.A. Minaeva, V.K. Popov, A.V. Popova. *Adv. Laser*, **1486**, 69 (2012). DOI:10.1063/1.4757825
- [10] R.K. Kankala, Y.S. Zhang, S.-B. Wang, A.-Z. Chen. *Adv. Healthc. Mater.*, **6** (16), 1700433 (2017). DOI:10.1002/adhm.201700433
- [11] K.M. Shakesheff, S.M. Howdle, M. Whitaker, R. Quirk. *J. Pharm. Pharmacol.*, **53** (11), 1427 (2001). DOI:10.1211/0022357011777963
- [12] P. Netti. *Biomedical Foams for Tissue Engineering Applications*, 1st ed. (Woodhead Publishing, Sawston, 2014)
- [13] A. Salerno, S. Zeppetelli, D.E. Maio, S. Lannace, P.A. Netti. *Compos. Sci. Technol.*, **13** (70), 1838 (2010). DOI: 10.1016/j.compscitech.2010.06.014
- [14] S.N. Swain, S.M. Biswal, P.K. Nanda, P.L. Nayak. *J. Polymer Environ.*, **12**, 35, (2004). DOI:10.1023/B:JOOE.0000003126.14448.04
- [15] M. Karimi, M. Heuchel, T. Weigel, M. Schossig, D. Hoffmann, A. Lendlein. *J. Supercrit. Fluids*, **61**, 175 (2012). DOI:10.1016/j.supflu.2011.09.022
- [16] Electronic source. Available at: <https://webbook.nist.gov/chemistry/fluid>
- [17] T. Lu, Y. Li, T. Chen. *Intern. J. Nanomedicine*, **8**, 337 (2013). DOI:10.2147/IJN.S38635
- [18] A. Taberero, L. Baldino, S. Cardea, E. Martín del Valle, E. Reverchon. *Polymers*, **11** (3), 485 (2019). DOI 10.3390/polym11030485
- [19] D. Zimnyakov, R. Zdrajevsky, N. Minaev, E. Epifanov, V. Popov, O. Ushakova. *Polymers*, **12** (5), 1055 (2020). DOI: 0.3390/polym12051055
- [20] D. Zimnyakov, M. Alonova, E. Ushakova. *Polymers*, **13** (7), 1115 (2021). DOI: 10.3390/polym13071115
- [21] D. Zimnyakov, M. Alonova, E. Ushakova, O. Ushakov, A. Isaeva, E. Isaeva. *Photonics*, **8**, 549 (2021). DOI:10.3390/photonics8120549
- [22] A. Ishimaru. *Propagation and Scattering of Waves in Random Media* (Academic, NY, 1978), v. 1.
- [23] D.A. Zimnyakov, S.A. Yuvchenko, A.A. Isaeva, E.A. Isaeva, O.V. Ushakova. *Opt. Spectr.*, **125**, 795 (2018). DOI: 10.1134/S0030400X18110371
- [24] M.U. Vera, A. Saint-Jalmes, D.J. Durian. *Appl. Opt.*, **40** (24), 4210 (2001). DOI: 10.1364/AO.40.004210
- [25] F.C. MacKintosh, S. John. *Phys. Rev. B*, **40** (4), 2383 (1989). DOI:10.1103/PHYSREVB.40.2383
- [26] G. Maret, P.E. Wolf. *Z. Phys. B Condens. Matter.*, **65**, 409 (1987). DOI: 10.1007/BF01303762
- [27] D.A. Zimnyakov, M.A. Vilensky. *Opt. Lett.*, **31** (4), 429 (2006). DOI: 10.1364/OL.31.000429
- [28] D.J. Pine, D.A. Weitz, P.M. Chaikin, E. Herbolzheimer. *Phys. Rev. Lett.*, **60**, 1134 (1988). DOI:10.1103/PhysRevLett.60.1134
- [29] S.S. Volchkov, I.O. Slavnetskov, A.V. Kalacheva, A.Sh. Gubanov, D.A. Zimnyakov. *Pisma v ZhTF*, **48** (17), 41 (2022). (in Russian). DOI: 10.21883/PJTF.2022.17.53287.19257
- [30] N.M. Lawandy, R.M. Balachandran, A.S.L. Gomes, E. Sauvain. *Nature*, **368** (6470), 436 (1994). DOI: 10.1038/368436a0
- [31] M.A. Noginov. *Solid-State Random Lasers* (Springer, NY, USA, 2005), DOI: 10.1007/b106788
- [32] V.S. Letokhov. *Sov. Phys. JETP*, **26** (4), 835 (1968).
- [33] A.S. Gittings, R. Bandyopadhyay, D.J. Durian. *Europhys. Lett.*, **65** (5), 414 (2004). DOI: 10.1209/epl/i2003-10084-4

Translated by Ego Translating